

JRC2012-74087

CRIPPLING TEST OF A BUDD PIONEER PASSENGER CAR

**Michael Carolan
Benjamin Perlman
David Tyrell**

Volpe National Transportation Systems Center
US Department of Transportation
Cambridge, MA 02142

ABSTRACT

This research program was sponsored by the Federal Railroad Administration (FRA) Office of Research and Development in support of the advancement of improved safety standards for passenger rail vehicles. FRA and the Volpe National Transportation Systems Center (Volpe Center) have conducted a research program to develop alternative methods for demonstrating occupied volume integrity (OVI) of passenger rail cars using a combination of testing and analysis. Previous publications have addressed the planning and progress of a series of tests intended to examine the collision load path through the occupant volume of passenger cars equipped with crash energy management (CEM) systems. This program has included an elastic 800-kip buff strength test, two quasi-static tests that loaded a passenger car to its ultimate (crippling) capacity, and corresponding finite element (FE) analyses of each test. This paper discusses the two crippling tests and the companion FE analyses.

One alternative method for evaluating OVI moves the applied loads from the line of draft to the collision load path. This alternative methodology also permits a combination of testing and analysis to be used to demonstrate the car's OVI, in contrast to the conventional methodology (as prescribed in existing FRA regulations) which only permits testing. The alternative methodology was adopted as the recommendations developed by the Railroad Safety Advisory Committee's (RSAC) Engineering Task Force (ETF) in its "Technical Criteria and Procedures for Evaluating the Crashworthiness and Occupant Protection Performance of Alternatively-Designed Passenger Rail Equipment for Use in Tier I Service." The research program was undertaken to verify the efficacy of using a combination of elastic testing and plastic analysis to evaluate the OVI of a passenger car loaded along its collision load path as prescribed in the ETF report.

Earlier in this research program an elastic test of a Budd Pioneer car was used to validate an FE model of the car, per the

ETF's procedures. This model was then modified to reflect the condition of the car in its crippling test configuration. The model was used to simulate the crippling behavior of the car, following the ETF's procedures. Two Pioneer cars were then tested to crippling to provide additional data to validate the FE model and the proposed alternative OVI evaluation.

Because the test cars used in this research program were equipped with CEM systems, the alternative evaluation loads were placed at the locations where the energy-absorbing components attached to the occupant volume. During both crippling tests, loads were measured at each energy-absorber support location on the live and restrained ends of the car. Additional instrumentation used in the second crippling test included strain gages on the major longitudinal structural members, displacement transducers at each load location, and vertical, lateral, and longitudinal displacement transducers on the underframe of the car. The results of the FE analysis compare favorably with the results of the crippling tests. In particular, the crippling loads are consistent between the tests and analysis: crippling loads for the first and second cars tested were 1.15 and 1.19 million pounds respectively, and the pre-test FEA estimated a crippling load of 1.19 million pounds. The research program has established a technical basis for the alternative OVI requirements and methodology.

INTRODUCTION

This research program was sponsored by the FRA Office of Research and Development in support of the advancement of improved safety standards for passenger rail vehicles. FRA is responsible for promulgating regulations to ensure the safety of railroad equipment traveling on the general railroad system in the U.S. Several regulations specify design requirements for particular structures within the passenger railcar. One such requirement is found at 49 CFR 238.203, "Static End Strength," commonly referred to as the "buff strength requirement." This part requires that

“...all passenger equipment shall resist a minimum static end load of 800,000 pounds applied on the line of draft without permanent deformation of the body structure.” [1]

FRA and the Volpe Center have worked to develop alternative strategies for evaluating occupied volume integrity (OVI) in passenger railcars [2]. This work was intended to help ensure the adequacy of the OVI of passenger railcars that are not designed to meet the requirements of the regulation. The results of this work were utilized by the RSAC’s ETF, which developed a set of guidelines for evaluating alternatively-designed passenger rail equipment. These guidelines, entitled “Technical Criteria and Procedures for Evaluating the Crashworthiness and Occupant Protection Performance of Alternately-Designed Passenger Rail Equipment for Use in Tier I Service,” are intended to be applied when presenting technical information in support of a request for a waiver of the current regulations [3].

Criteria and Procedures

The ETF has adopted three sets of criteria (referred to as options) for evaluating OVI. Each option includes an evaluation load magnitude and a corresponding pass-fail criterion. A passenger car may demonstrate its OVI by meeting any of the three options. The three options are summarized in Table 1.

Table 1. ETF Criteria Options

	Load Magnitude (pounds)	Pass-fail Criterion
Option A	800,000	No permanent deformation
Option B	1 million	Limited permanent deformation
Option C	1.2 million	Without crippling

The ETF has also developed a set of procedures used to evaluate each of the three options. The full details of the procedures can be found in the ETF’s report [3]. When evaluating any of the three options, the evaluation load is placed on the car structure along the path taken by the collision loads. This load path will vary from car design to car design, and must be determined on a vehicle-by-vehicle basis. The procedures permit a combination of elastic testing and plastic analysis to be used to determine whether a design meets the ETF’s criteria. The results of the elastic test may be used to validate an FE model of the car structure undergoing evaluation. Once properly validated, the FE model can be used to evaluate the response of the railcar to a load greater than that which was applied in the elastic test for any of the three options.

TESTING PROGRAM

A series of tests was developed to evaluate the loading conditions as well as the procedures developed by the ETF. The tests performed in this program were conducted by Transportation Technology Center, Inc. (TTCI) in Pueblo, CO. The overall strategy for performing the tests was presented in a 2009 paper by Carolan and Muhler [7]. The strategy called for demonstrating the load capacity of an existing 800,000 pound compliant passenger car along an alternative load path by loading the car at its floor and roof levels. The car design selected for this program was a Budd Pioneer passenger car. An initial 800,000 pound compression test was performed in January, 2010 and discussed in Reference 4. Due to uncertainties in the results of this test and the discovery of localized damage to the test car, a second 800,000 pound compressive strength test was conducted on January 19, 2011 [8]. This test verified that the car was in a suitable condition to be used as the test article in the crippling test. The data collected during this elastic test was then used to validate a structural FE model of the Budd Pioneer passenger car. The results of the elastic test, analysis results, and a comparison of key measurements can be found in Reference 8. The validated FE model was then able to be used to simulate the response of the Pioneer car up to its crippling load.

Test Articles

As a part of a previous FRA research program, conventionally-designed passenger railcars were retrofitted to include CEM components [5]. Because these cars were originally built for service in the U.S., each car was capable of meeting the 800,000 pound buff strength requirement. Service loads were transmitted along the line-of-draft even after the CEM systems were installed. In the event of a collision, however, the collision loads followed a different path through the structure. The collision loads were transmitted through the energy-absorbing elements and into the occupant volume. In this particular design, the collision loads are shared between energy-absorber supports at the floor-level and at the roof-level.

Two CEM-equipped railcars were used in the current research program’s tests. These cars were Budd Pioneer cars 244 and 248. The CEM-equipped Pioneer was selected for this program for several reasons. Because the occupant volume was originally constructed to meet the 800,000 pound buff strength requirement, this car’s structure represents the load-bearing capability of a conventionally-designed passenger car. The CEM elements of this design move the collision loads away from the line of draft, permitting the ETF’s evaluation methodology to be applied along the collision load path. This car’s design permits the new methodology to be used to examine the performance of a car known to meet the conventional requirement. Budd Pioneer 244, with its CEM structures installed, is shown in Figure 1.



Figure 1. Budd Pioneer 244 with CEM

Following the elastic test of Car 244, preparations began for the crippling test of this car. In the crippling test, the loads were introduced into the car along its collision load path. Because of the CEM components installed on this design the collision loads do not travel along the line of draft. This particular design features two roof-level and two floor-level energy absorber supports at the ends of the occupant volume. In the event of a collision, loads are transmitted from the end frame into the energy-absorbing components. The energy absorbers transfer their loads through the four supports on each end of the occupant volume. The loads then travel through the occupant volume and out through the energy absorbers at the rear end of the car.

In order to access the energy-absorber supports, the end frames were removed from both ends of both Pioneer cars. Additionally, the energy-absorbing components were removed. Figure 2 shows the end of Pioneer car 248 with its end frame removed. The four energy-absorber support locations are indicated in this figure.

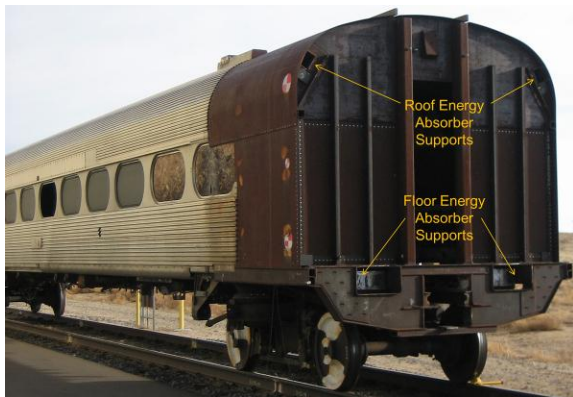


Figure 2. Pioneer 248 with End frame Removed

Test Setup and Conduct

The 800,000 pound elastic test of car 244 was conducted in the conventional manner. The car was loaded and restrained along its line-of-draft and a maximum compressive load of 800,000 pounds was applied. The details of this test, its instrumentation, and its results may be found in Reference 8.

The crippling tests required departure from the conventional method used to conduct the elastic test. A test frame capable of reacting loads at different heights was needed to load and restrain the car at roof- and floor-level locations. Additionally,

a system capable of simultaneously introducing load into the structure at four different locations was also required as well as a control system capable of maintaining equal displacements in each of the live end loading actuators.

The frame used to restrain the car during both crippling tests is made up of four longitudinal beams: two at the roof-level and two at the floor-level. The four beams are supported by a series of vertical beams and span the length of the car. The two longitudinal beams at a given height are attached to one another by a lateral support at each end of the car. The live end of the frame is attached to the ground, but the back end is free to move longitudinally. Based upon the load path through the car and into the frame, the four longitudinal beams will stretch in response to loads being transmitted into them by the car. The test frame, with Car 244 installed within it, is shown in Figure 3. Three of the loading locations on the live end are indicated in this figure, as are three reaction locations on the back end of the car.



Figure 3. Crippling Test Frame with Car 244

Two crippling tests were performed by TTCI: a limited-instrumentation “shakedown” test of car 248 and a fully-instrumented test of car 244. The limited-instrumentation test was performed as a shakedown of the newly-installed load frame and hydraulic control system. Car 248 was selected for the shakedown test because areas of damage from a previous impact testing program had been identified. While the car’s structure was mostly intact, it was thought the damage could influence the crippling load magnitude and the failure mode. Having successfully demonstrated its structural integrity in an 800,000 pound elastic test, car 244 was used in the fully-instrumented crippling test.

In both tests, load was applied to the car in a series of 200-kip increments. For loads up to 800 kips the load was removed between load cycles. Once a load of 800 kips was reached the load was not removed from the car until crippling occurred. The maximum loading rate applied during the test of Car 244 was 0.13 inches per second. Generally, the load rate was less than 0.05 inches per second.

This material is declared a work of the U.S. Government and is not subject to copyright protection in the United States. Approved for public release; distribution is unlimited.

Instrumentation

During both crippling tests, the pressure and displacement of each hydraulic actuator at the live end of the car were measured. Load cells were used to measure the load applied to each location on the live end of the car. Load cells were also used to measure the reaction load at each restraint location on the rear end of each car in both crippling tests.

In the fully-instrumented test of car 244, the instrumentation included strain gages installed on key longitudinal members of the carbody structure. String potentiometers were installed between the underframe of the car and ground. Longitudinal string potentiometers were also installed between the reaction locations at the back end of the car and ground. Table 2 is a summary of the data channels used in the fully-instrumented test.

Table 2. Instrumentation from Crippling Test of Car 244

Type of Instrumentation	Number of Channels
Uniaxial Strain Gage	76
String Potentiometer	41
Load Cell	8
LVDT	4
Pressure Transducer	4
Temperature	1
Total	134

Strain gages were installed at six cross-sections of car 244 during the crippling test. Arrays of vertical, lateral, and longitudinal string potentiometers were installed at 11 locations on the underframe of the car. As explained in Reference 8, the use of this string pot arrangement permitted the measurements at each point to be resolved into displacements in each of the three directions. The string pot and strain gage locations are shown schematically in Figure 4.

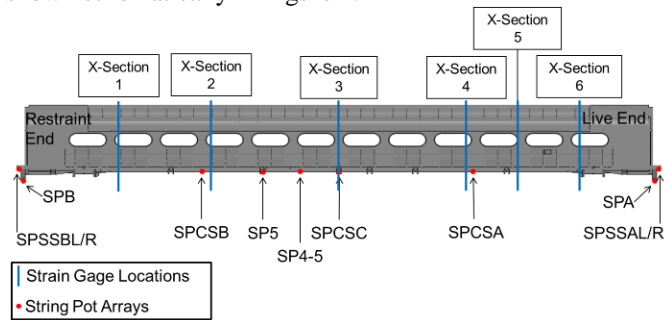


Figure 4. Strain Gage and String Pot Locations in Fully-Instrumented Crippling Test

Load Cells

The occupant volume of the car was loaded at four locations in this test: two floor-level energy absorber supports and two roof-level energy absorbers. The hydraulic system used in the crippling test was capable of maintaining an equal displacement in each of the four hydraulic actuators loading the live end of the car. This loading scheme was used in both

cripling tests. At the back end of the car, the car was restrained by the frame at the corresponding four energy-absorber supports.

Eight load cells were used to measure the individual loads being placed on the car as well as to examine the load path through the structure of the car. A load cell with a capacity of 1,000,000 pounds was placed between each floor energy-absorber support and the test frame on both the live and back ends of the car. A 500,000-pound capacity load cell was installed between each roof energy-absorber support and the test frame. Figure 5 shows the restraint arrangement at the roof-level at the back end of the car. The car is at the right side in this photograph, the load cell in the center, and the lateral component of the test frame at the left side.

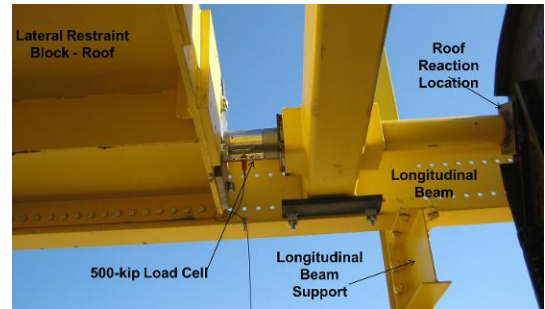


Figure 5. Roof Reaction Location at Back End of Car, Crippling Test

Strain Gages

Uniaxial strain gages were used to instrument the car at six cross-sections. At sections one through five, gages were applied to the center sill, side sills, belt rails, roof rails, and purlins. At location six, strain gages were only used on the side sill and belt rail. Figure 6 shows a cross-section of the car taken from the FE model. The members that were instrumented with strain gages are indicated in this figure. The placement of the strain gages on the cross-section of each member is indicated by the sketches on the left side of this figure.

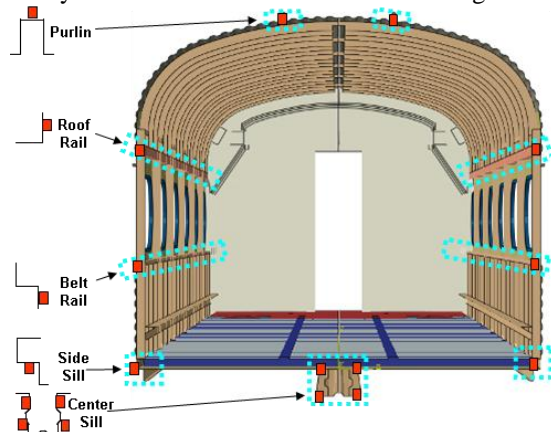


Figure 6. Cross-section of Pioneer 244 Showing Strain Gages in Crippling Test

Additional strain gages were installed in the vicinities of the load and restraint locations. On the underside of the car, strain gages were added to the energy absorber support structure. At the roof level, strain gages were added to the roof structure surrounding the support tube for the roof energy absorber.

FE MODEL

The crippling test was simulated using the commercial finite element software Abaqus/Explicit [6]. An explicit finite-element solver was chosen for the analysis because of the expectation of large deflections and of the need to capture the buckling behavior as the model experienced crippling. A slowly-applied dynamic load served as an approximation of the quasi-static test condition.

A half-symmetric (full length, half width) FE model was used to simulate the 800,000 pound buff strength test. This model is shown in Figure 7. This FE model had been derived from previous Budd Pioneer FE models used to simulate a series of dynamic impact tests [7]. The results of this model were in sufficient agreement with the results of the 800,000 pound line-of-draft test for the model to be considered validated [8].

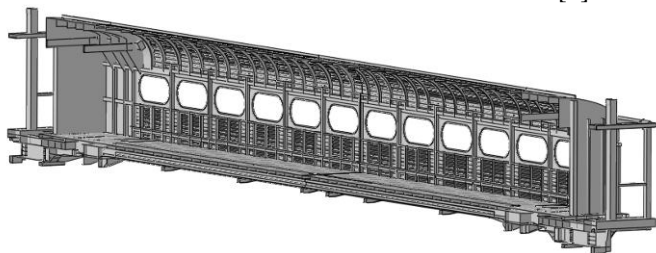


Figure 7. Half-symmetric FE Model Used in 800-kip Buff Strength Analysis

This validated model was used as the starting point to create the crippling model. Because the endframes and CEM components were removed from both Pioneer cars to permit loading along the collision load path in the crippling tests, these structures were removed from the crippling FE model as well. Additionally, because the lateral-vertical symmetry used in the 800-kip model could suppress a lateral buckling mode in the crippling model, the existing structure was mirrored to create a full-car model. The crippling analysis model is shown in Figure 8.



Figure 8. FE Model Used in Crippling Analysis

This material is declared a work of the U.S. Government and is not subject to copyright protection in the United States. Approved for public release; distribution is unlimited.

Materials

This FE model was derived from previous models used to simulate dynamic impact tests. The crippling model was originally constructed to simulate an impact test of a conventional Pioneer car [9]. When the car itself was modified to include CEM components a CEM-retrofitted model was created [10]. The crippling model used this existing CEM model as a starting point. The elastic-plastic material properties that were already defined for the materials in this car were used for the crippling analysis.

This car includes several different types of steel in its structure. A simple bi-linear material representation was used for most strength properties defined in the FE model. The first portion of the material property definition represents the elastic response of the material up to its yield strength. The second portion of the material property definition represents the plastic behavior of the material between its yield strength/strain and its ultimate strength/strain. No attempt was made to include fracture or material softening in this model. Bi-linear material behavior is shown schematically in Figure 9.

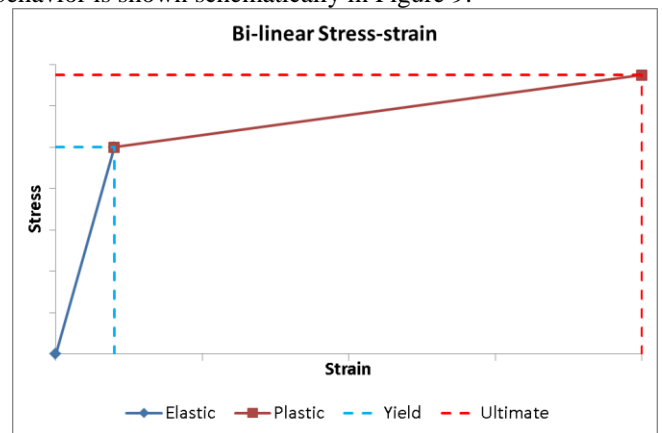


Figure 9. Schematic of Bi-linear Representation of Material Strength Property

Mesh

The crippling analysis model contained 366,527 nodes and 374,506 elements. The vast majority of these elements were shell elements. Specifically, 365,334 S4R elements were used in this model. This element is a 4-noded reduced integration shell [6]. A total of 2,220 triangular S3R shells were used in the body structure. Of the remaining elements 4 were non-linear spring elements used to simulate the behavior of the suspension, connecting the car body to ground. The areas around the window openings and in the purlins at the ends of the car were modeled using 6,924 C3D8R brick elements. The mesh had a characteristic element length of 1.44 inches. The body shell in the model had a weight of approximately 28,100 pounds.

Boundary Conditions

Because the FE model that was used to simulate the 800,000 pound test was used as a starting point for the crippling model, the boundary conditions are substantially the same in both models. The boundary conditions placed on the 800,000 pound model are discussed in detail in Reference 8. Because the crippling model was a full-length and full-width model, no symmetry boundary condition was used. Vertical springs were modeled at each of the four body bolster locations where the trucks would interface with the physical car body. The grounded end of each spring was free to move in the longitudinal direction, simulating the freedom of the physical truck to roll on the track.

Four energy-absorber supports on the live end of the car were used as loading locations. The corresponding locations on the back end were used to restrain the car in the longitudinal direction. Load was introduced into the FE model by prescribing a 2 inch/second displacement on a row of nodes at the center of each floor- and roof-level energy absorber support. At the rear (reaction) end of the car, a similar row of nodes at each energy-absorber location was prevented from moving in the longitudinal location. Applying the boundary condition to a single row of nodes allowed each location to pivot in response to the applied or reacted load. These locations are indicated on the FE model in Figure 10.

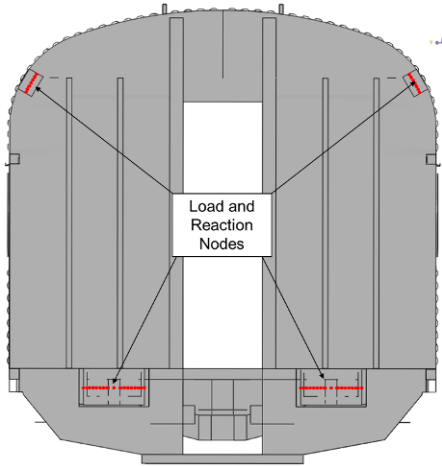


Figure 10. Load and Reaction Locations on FE Model

The boundary conditions placed on the back end of the FE model prevent the reaction locations from displacing longitudinally, thus restraining the car. However, in the physical tests the support frame is free to stretch in response to the reaction loads at the back end of the car. The stroke length measured in each hydraulic actuator on the live end of the car includes compression of the car within the frame as well as stretching of the test frame itself. The displacement of the back end of the car must be subtracted from the actuator stroke to obtain the overall change in car length before the load-

displacement results from the FEA and the test can be compared.

RESULTS – CRIPPLING TESTS AND ANALYSIS

Verification of Quasi-static Behavior

In the ETF's report, two criteria are established for determining whether a slowly-applied dynamic load is sufficiently free from dynamic effects to be considered quasi-static. While an analysis must only meet one of the two criteria to be considered quasi-static, both methods of evaluation were used to examine the FE model in this research program.

ETF Condition One

For a given simulated load rate, the load at the live end of the model should be the same as the load at the fixed end. Load at the reaction end may vary by up to +/- 5% of the load at the live end of the model for the analysis to be considered quasi-static [3].

A displacement boundary condition was used to apply loads to the four live-end locations in the FE model. The FE software calculates the force that must be applied at each location to achieve the prescribed displacement. Similarly, at the back end of the car a zero-displacement boundary condition was enforced for longitudinal displacement at each reaction location. The FE software calculates the force that must be applied to maintain zero displacement at the selected locations.

The four loads applied to the live end were added together and plotted against the displacement of the live end. The four loads at the back end were also summed and plotted against the displacement of the live end. A +/- 5% envelope on the live-end force was plotted alongside the two load-displacement characteristics in Figure 11. This figure shows that the applied load and the reaction load are in close agreement. The model may be considered quasi-static by the first ETF criterion.

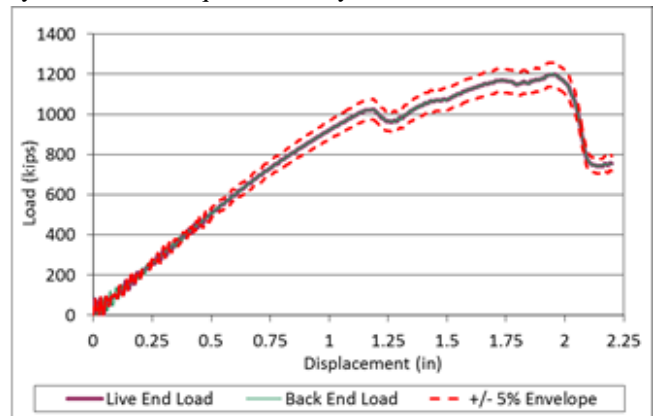


Figure 11. Live End Load and Back End Loads for Crippling Analysis

ETF Condition Two

The ratio of kinetic energy to strain energy within the structure should be small (<5%). The ratio of kinetic energy-to-strain energy may exceed 5% during the first 10% of the total simulation time without invalidating the analysis as quasi-static [3].

Because Abaqus/Explicit was used to evaluate the crippling load, a slowly-applied but dynamic load was introduced into the structure. The Abaqus solver can calculate the total kinetic energy of the system, as well as the internal (strain) energy. Because a model executed in this way initially experiences very little deformation, the ETF procedures permit the ratio of kinetic energy to internal energy to exceed 5% for the first 10% of the simulation time.

The energy ratio for the crippling simulation is plotted in Figure 12. The simulation consisted of two steps: a gravity step and a compression load step. The transition between the two steps is indicated by a dashed vertical line in this figure. The energy ratio is plotted on a logarithmic scale as this quantity varied by several orders of magnitude over the course of the simulation.

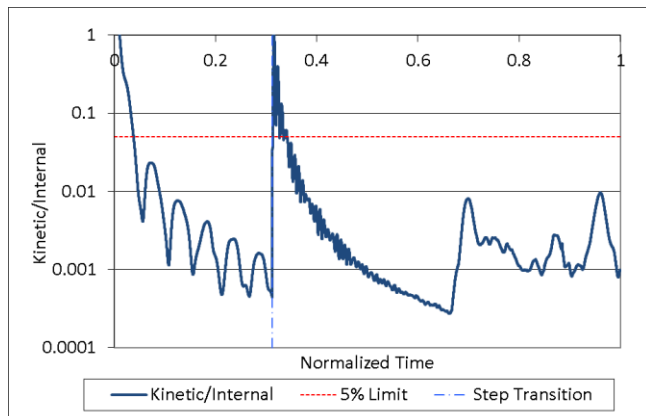


Figure 12. Ratio of Kinetic Energy to Internal Energy for Crippling Simulation

Figure 12 shows that the ratio of kinetic energy to internal energy was well below 5% for nearly the entire length of the simulation. Based upon this criterion, the crippling analysis can be considered quasi-static.

Load and Displacement Behavior

As a comparison between the test and the FE model results, the displacement measurements provide a global description of how well the model is capturing the test behavior. As the OVI evaluation is an assessment of the entire occupant volume's ability to support load, the global load versus displacement behavior is a critical measurement to be compared between test and model.

This material is declared a work of the U.S. Government and is not subject to copyright protection in the United States. Approved for public release; distribution is unlimited.

The load-versus-displacement behavior was measured in both crippling tests as well as the analysis. This behavior is a measurement of the global behavior of the car structure and its ability to support compressive loads. The load measurements can be made directly from the four load cells installed on the live end of the car during a crippling test. During its crippling test, car 244 was instrumented with string potentiometers measuring the longitudinal travel of the reaction end of the car. The change in car length can be determined by subtracting these displacements from the displacements at the live end. Because each reaction point could deflect by a different amount the four measurements for change in car length must be averaged to obtain the global shortening of the car.

Figure 13 contains a plot of the applied load versus the change in car length for car 244 during its crippling test. This figure includes a plot of the sum of the two floor-level live-end load cells, a plot of the sum of the two roof-level live-end load cells, and a plot of the sum of the four live-end load cells.

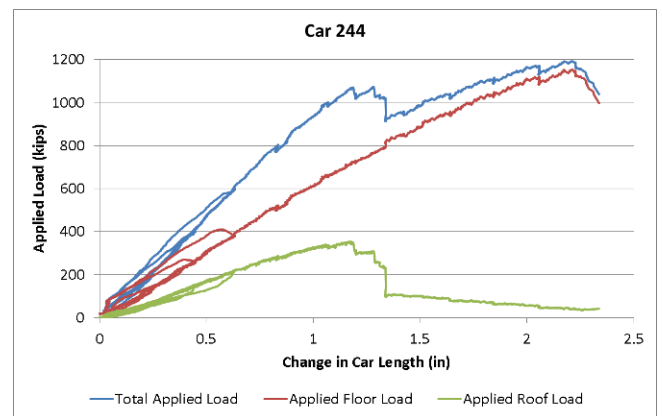


Figure 13. Applied Loads, Car 244 Crippling Test

As seen in the Figure 13, the roof structure carries a smaller load than the floor and buckles at a lower load. Once the roof has buckled the applied roof load quickly drops. The floor structure continues to carry load once the roof has buckled. When crippling is reached, nearly the entire load is entering the car structure through the floor-level energy-absorber supports.

Figure 14 contains a plot of the applied load versus change in car length for the FE analysis of the crippling test. Similar to Figure 13, this figure includes plots of the applied floor load, the applied roof load, and the total applied load. The horizontal axis represents the change in car length as calculated by the FE model. This is the same measurement as was used in Figure 13.

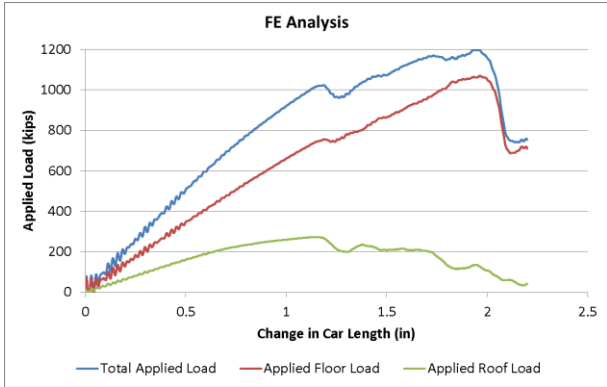


Figure 14. Applied Loads, FE Analysis

The load-versus-displacement behavior calculated by the FE model is similar to the measurements made during the test. In the FE model as well as the test, the roof's load-displacement curve has a lower slope than that for the floor, as well as a lower buckling load. The roof structure in the FE model buckles at a lower load than the roof structure in the test car. In the FE model, the roof undergoes more gradual buckling behavior than was experienced during the test, resulting in a less-abrupt drop in roof load.

The floor structure in the FE model behaves similarly to the floor structure in the test. At the time of crippling, the majority of the load supported by the car body is entering through the floor structure. However, in the FE model the roof is carrying more load than the roof in the test of car 244.

Because car 248 was tested in a limited-instrumentation "shakedown" test, displacement measurements were not made at the back end of the car. While displacement measurements were made at each hydraulic actuator on the live end, the stroke length of each actuator is a measurement of the compression of the car plus stretching of the test frame. Because car 244 was tested in the same frame, the live end actuator displacements from the two tests can be compared directly to one another. The total applied load in both test cars is plotted against the live end actuator displacements for cars 244 and 248 in Figure 15.

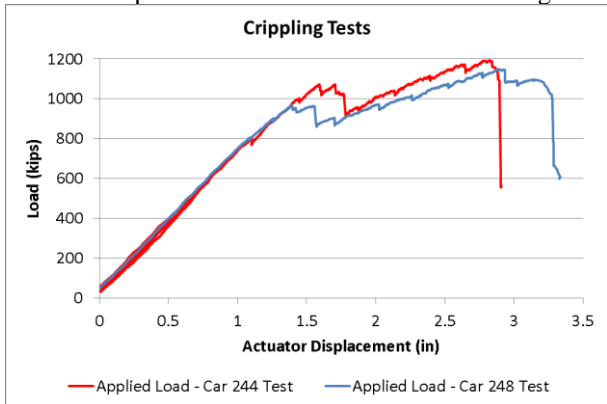


Figure 15. Load versus Actuator Displacement for Tests

Cars 244 and 248 experienced similar modes of deformation throughout the test. Both of the cars initially deformed in an approximately linear manner with increasing load. In both tests the roof buckled at a load of approximately 1-million pounds. Car 248's roof buckled at slightly less than 1-million pounds, and car 244's at slightly more. Following this buckling, the load continued to climb as the underframe continued to carry load. Crippling was reached when the center sill and side sills failed in buckling.

Because the FE model was fixed at its back end but the test car was restrained by a stiff but deformable frame, the live end displacement in the FE model is not the same as the live end displacement in the test. In the fully-instrumented test of car 244, the longitudinal displacement of each reaction location on the rear end of the car was measured. The shortening of the car itself was calculated by subtracting the rear end displacement from the live end displacement. Because of the limited instrumentation installed on car 248, the rear end displacement was not measured and car shortening cannot be determined. The load versus change in car length is plotted in Figure 16 for the test of car 244 and the FE analysis.

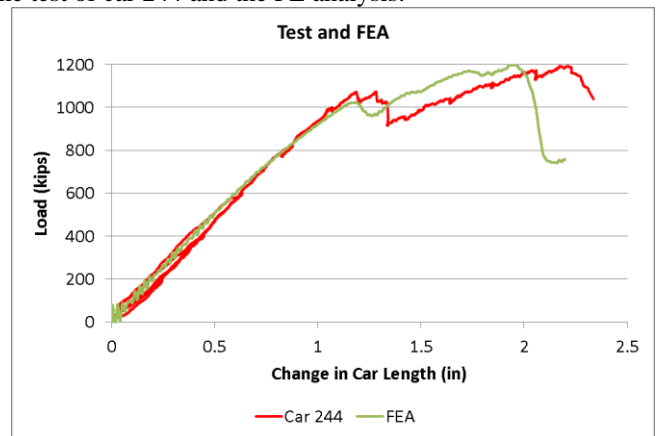


Figure 16. Load vs. Change in Car Length for Car 244 and FEA

The crippling behaviors observed in both tests and calculated by the FE model are largely the same. Car 248 reached a crippling load of 1.15 million pounds. Car 244 and the FE model both reached crippling loads of more than 1.19 million pounds.

Deformation Shape

Figure 17 is an image of the deformed shape predicted by the FE model. In this model, the roof buckled between the 6th and 8th windows from the live end of the car. The underframe (center and side sills) buckled beneath the 7th and 8th windows from the left. As can be seen in this figure, both the roof and underframe structures experienced a rather gradual large-scale buckle.

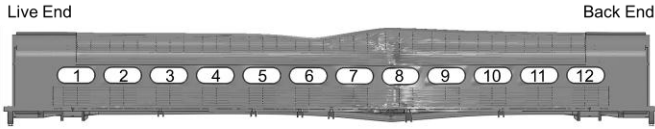


Figure 17. Post-crippling Deformed Shape Predicted by FE Model

Car 248 experienced roof buckling between the 7th and 8th windows from the live end of the car. The center sill of this car buckled in two locations. These two buckles were both located beneath the 8th window from the live end. The left and right side sills both buckled at locations between the 7th and 8th windows from the live end. A side view of Car 248 following its crippling test is shown in Figure 18. The roof and underframe buckles in this car were fairly localized.



Figure 18. Post-crippling Photograph of Car 248

Prior to performing any tests in this research program, the candidate test cars were inspected for their suitability for testing. Damage was discovered on car 248's floor and sidewall structures in the vicinity of the 7th and 8th windows from the live end. This damage likely acted as an initiation site for the buckling that occurred in the car during the crippling test. It is also likely that this preexisting damage is partially responsible for the slightly lower crippling load supported by car 248 compared to car 244.

Car 244 experienced the same sequence of buckling events as car 248, but at different locations along its length. Car 244's center sill buckled at two locations. Beneath the 1st window from the live end, the lower flange of the center sill buckled. Beneath the 3rd window the upper flange of the center sill buckled. The right and left side sills buckled under the 1st and 3rd windows, respectively. The sidewall and roof structures of Car 244 buckled between the 3rd and 5th windows. Car 244 is shown in Figure 19 in its post-crippling state. Similar to car 248, the damaged areas were fairly localized on car 244.



Figure 19. Post-crippling Photograph of Car 244

While the two tested cars experienced crippling at different locations along their lengths, the manner in which buckling progressed to crippling was substantially similar. Both cars first experienced a buckling of the roof structure at a load of approximately 1-million pounds. Following this buckling and

the corresponding drop in load the total load resumed its rise as the load carried by the underframe increased. The load-displacement characteristics from both cars possess similar slopes following the roof's buckling, as seen in Figure 15. Finally, the ultimate load for each car was reached when the center and side sills failed by buckling.

Strain Results

Strain gages were installed throughout the car as a means of examining the details of the car's behavior throughout the test. Each strain gage is capable of measuring highly localized behavior within the structure of the car. While strain gages were installed throughout the cross-section of the car, this car was designed to carry longitudinal loads in its center sill and side sills. These members are fairly large in cross-section compared with the other longitudinal members making up the structure of the car.

Strain gages were installed on car 244 on the members shown in Figure 6 at cross-sections 1 through 5 as shown in Figure 4. The bottom flange of the center sill buckled at approximately cross-section 5. While the center sill experienced buckling in the upper web at a different location, the lower flange buckle was very close to several strain gages. This buckle and two strain gages installed on the center sill are shown in Figure 20. The lower flange of the center sill features an additional plate welded to its top surface toward the live end of the car that terminates at this cross-section. In this photograph the live end of the car is to the left hand side.



Figure 20. Buckle in Lower Flange, Center Sill of Car 244

Each center sill cross-section that was instrumented with strain gages included an upper and a lower gage on each side, for a total of four gages. Because the buckle in the lower flange in car 244 was roughly the same shape across the entire width of the center sill both the lower left and lower right gages recorded very similar behavior. The strain measured by each of the four gages is plotted against the total applied load in Figure 21.

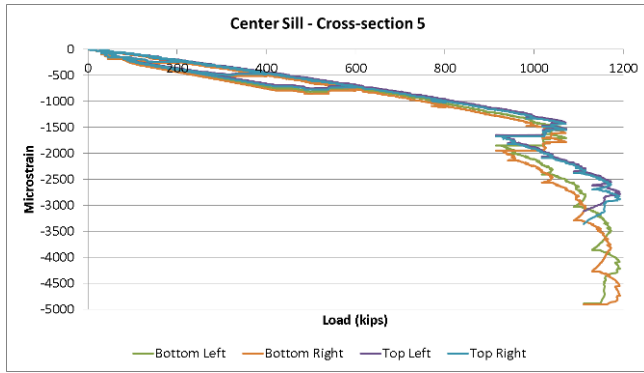


Figure 21. Strain vs. Load for Center Sill of Car 244 at Buckled Lower Flange

The strains measured in the center sill are roughly linear with respect to the applied load up to a load of approximately 1-million pounds. This load correlates with the approximate load at which the roof of the car buckled. Beyond 1-million pounds the lower strain gages experience a more rapid change in strain for a given change in load than the two upper strain gages. The strain gages used in the crippling test of Car 244 had a measurement capacity of +/- 3,000 microstrain.

In the FE model, the center sill buckled closer to the center of the car (see Figure 17). The center sill in the FE model experienced a buckling of the upper flanges and webs. Figure 22 shows a close-up view of the buckled center sill and side sill in the FE model.

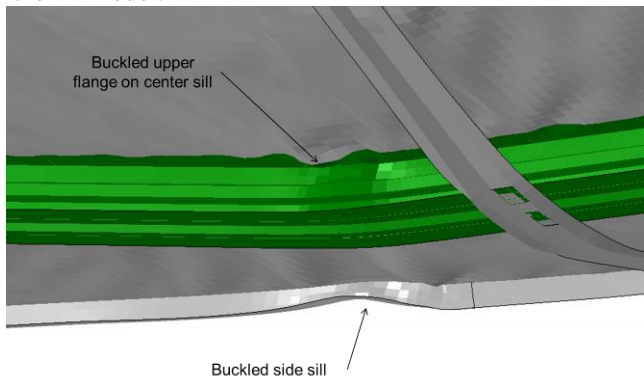


Figure 22. Buckled Center Sill in FE Model

Field data were collected in the vicinity of the buckle during the crippling analysis. Figure 23 plots the strains in the center sill at the buckling location. The four data series shown in this figure are for elements in locations that correspond to the approximate placement of strain gages on the cross-section of car 244's center sill.

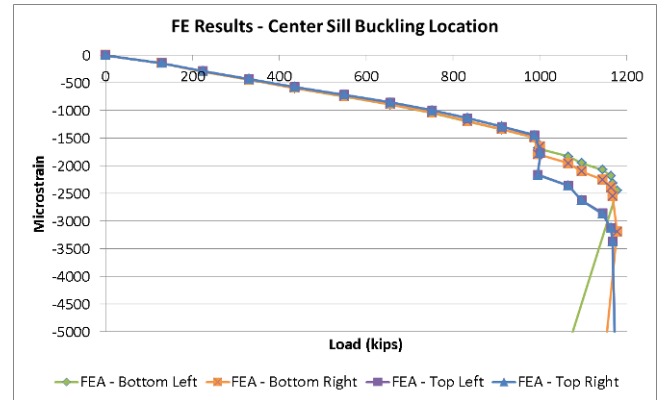


Figure 23. Strain vs. Load for Center Sill of FE Model at Buckled Location

The strain behavior in the FE model in the vicinity of the center sill's buckle is similar to the behavior seen in car 244. The four gages register approximately the same strain for a given load up to approximately 1-million pounds. Because the center sill in the model buckles at the top, the two calculated locations closer to the top indicate a faster rate of change of strain per change in applied load than the two locations at the bottom.

CONCLUSIONS

A series of quasi-static tests and analyses has been undertaken to evaluate the ETF's recently-developed criteria and procedures for evaluating the OVI of passenger railcars. This research program applied the ETF's criteria and procedures to a passenger railcar to evaluate the efficacy of the new methodology. The ETF's methodology was applied through quasi-static testing and FE analyses of an 800,000 pound compliant passenger car that had been retrofitted with CEM structures.

Following the ETF's methodology, a conventional 800,000 pound elastic line of draft loading was used to validate an FE model of the Pioneer car. The validated model was then used to simulate loading of the car along its collision load path until its crippling load was reached. Exceeding the ETF's requirements, two Pioneer cars were destructively tested to the point of crippling.

The results of the crippling FE analysis were compared with the results of the two crippling tests. The longitudinal load versus displacement behavior of the two test cars and the FE model agree closely for loads up to more than 800,000 pounds. In both tests and in the model, the crippling sequences are similar. Buckling of the roof occurred in all three cases at a load of approximately 1-million pounds. Following the roof buckling, the underframe continued to bear load until crippling was reached. The crippling loads in each of the three cases were similar. Pioneer 248 crippled at a load of 1.15 million pounds, Pioneer 244 at 1.19 million pounds, and the FE model at 1.19 million pounds. This research program has

demonstrated a sound technical basis for the criteria and procedures developed by the ETF.

ACKNOWLEDGEMENTS

This work was performed by the Volpe Center as part of the Equipment Safety Research Program sponsored by the Office of Research and Development of the Federal Railroad Administration. Mr. Kevin Kesler is Chief of the Equipment and Operating Practices Division. Ms. Melissa Shurland and Mr. Jeff Gordon were the Program Managers for the Passenger Equipment Safety Research Program during this research. Mr. Luis Maal is the FRA resident manager of the Transportation Technology Center (TTC) in Pueblo, CO. The full-scale testing, instrumentation installation and documentation of the tests were performed by Transportation Technology Center, Inc. The Budd Pioneer cars utilized in this research program were donated by SEPTA. The assessment criteria and procedures applied to the test car were developed by the RSAC's ETF. Ms. Michelle Muhlanger, Volpe Center, helped implement the 800,000 pound elastic test.

REFERENCES

1. *Static End Strength*, 49 CFR 238.203.
2. Carolan, M., Perlman, B.A., Tyrell, D., "Evaluation of Occupant Volume Strength in Conventional Passenger Railroad Equipment" American Society of Mechanical Engineers, Paper No. RTDF2008-74026, September 2008.
3. "Technical Criteria and Procedures for Evaluating the Crashworthiness and Occupant Protection Performance of Alternatively Designed Passenger Rail Equipment for Use in Tier I Service," U.S. Department of Transportation Report No. DOT-FRA-ORD-11/22. Washington, DC: Federal Railroad Administration, Office of Railroad Policy Research and Development, October 2011.
4. Carolan, M., Muhlanger, M., "Update on Alternative Occupant Volume Testing," American Society of Mechanical Engineers, Paper No. JRC2010-36020, April 2010.
5. Mayville, R., Rancatore, R., Stringfellow, R., and Amar, G., "Repair of Budd Pioneer Coach Car Crush Zones." U.S. Department of Transportation, DOT/FRA/ORD-07/18, May 2007.
6. Dassault Systèmes, 2010. Abaqus/Explicit 6.10-1. Providence, RI, USA.
7. Carolan, M., Muhlanger, M., "Strategy for Alternative Occupant Volume Testing" American Society of Mechanical Engineers, Paper No. RTDF2009-18025, October 2009.

-
8. Carolan, M., Muhlanger, M., Perlman, B., and Tyrell, D. "Occupied Volume Integrity Testing: Elastic Test Results and Analyses." American Society of Mechanical Engineers, Paper No. RTDF2011-67010., September 2011.
 9. Kirkpatrick, S., and MacNeil, R. "Development of a Computer Model for Prediction of Collision Response of a Railroad Passenger Car." Proceedings of the 2002 IEEE/ASME Joint Railroad Conference, Institute of Electrical and Electronics Engineers, Catalog Number CH37356-TBR, 2002.
 10. Jacobsen, K., Tyrell, D., and Perlman, A.B. "Impact Test of a Crash-Energy Management Passenger Rail Car." American Society of Mechanical Engineers, Paper No. RTD2004-66045, April 2004.

This material is declared a work of the U.S. Government and is not subject to copyright protection in the United States. Approved for public release; distribution is unlimited.